

Dynamics and transformations of Josephson vortex lattice in layered superconductors

D.A.Ryndyk, V.I.Pozdnjakova, I.A.Shereshevskii, N.K.Vdovicheva

Institute for Physics of Microstructures, Russian Academy of Sciences

*GSP-105, Nizhny Novgorod 603600, Russia**

(Dated: 25 of April, to be published in Phys. Rev. B)

Abstract

We consider dynamics of Josephson vortex lattice in layered superconductors with magnetic, charge (electrostatic) and charge-imbalance (quasiparticle) interactions between interlayer Josephson junctions taken into account. The macroscopic dynamical equations for interlayer Josephson phase differences, intralayer charge and electron-hole imbalance are obtained and used for numerical simulations. Different transformations of the vortex lattice structure are observed. It is shown that the additional dissipation due to the charge imbalance relaxation leads to the stability of triangular lattice.

PACS numbers: 74.50.+r, 74.80.Dm, 74.72.-h

*Electronic address: ryn@ipm.sci-nnov.ru

The investigation of the resistive state of layered high- T_c superconductors in the external magnetic field parallel to the layers is the important task of modern experiment and theory. The c -axis resistivity in this case is determined by Josephson flux flow. Thus, the nonstationary properties of HTSC can be investigated in wide parameter range of temperatures, fields and currents. In the recent experiments [1, 2, 3, 4] flux flow states in low magnetic fields are observed and in Ref. [5, 6] – in high fields up to 3.5 T. The number of peculiarities is discovered. In particular, in Ref. [2, 4] multiple flux flow branches, associated with different vortex modes, are observed. In Ref. [3, 4] it is shown that two universal flux flow regimes with different V/H take place at different magnetic fields and transformation from the first state to the second is possible with current rise at intermediate fields. Finally, in Ref. [6] broad-band microwave emission is measured with frequencies much less than Josephson frequency $\omega_J = 2eV/N\hbar$. All this phenomena are related to the dynamical transformations of Josephson vortex lattice (JVL) and vortex interaction with linear plasma modes (see also Ref. [7, 8, 9, 10, 11, 12, 13, 14, 15, 16, 17]).

On the other hand, there is the long-standing problem to obtain the coherent electromagnetic emission from stacked Josephson junction. The most simple way to do this is to achieve "in-phase" (square) arrangement of vortices. Although at zero external current the triangular JVL is favorable, it was shown for two-junction stack theoretically and experimentally [11, 14] and for multi-junction stack theoretically [9, 10, 13, 15, 16] that moving square JVL can be stable. However no indications of this in-phase regime were found in experiments with HTSC. The reason for this discrepancy may be that only magnetic coupling between layers have been taken into account in calculations.

In [18, 19, 20, 21, 22, 23] it was also suggested that in the case of thin superconducting layers some nonequilibrium mechanisms are to be taken into account, namely electrical charging of layers (charge effect) and nonequilibrium quasiparticles (charge-imbalance effect). To investigate this effects we obtain macroscopic dynamical equations for interlayer Josephson phase differences with magnetic, charge and charge-imbalance interactions taken into account.

Following [7, 8] we use London expression for the longitudinal in-layer supercurrent neglecting longitudinal in-layer electric field \mathbf{E}_n^{\parallel} and normal current (with accuracy

$(\sigma_{ab}/\sigma_c)\gamma^{-2} \ll 1$, $\gamma = \lambda_c/\lambda_{ab}$ is the anisotropy parameter)

$$\mathbf{j}_n^{\parallel}(\mathbf{r}) = -\frac{c\Phi_0}{8\pi^2\lambda^2} \left[\nabla_{\parallel}\theta_n(\mathbf{r}) + \frac{2\pi}{\Phi_0}\mathbf{A}_n(\mathbf{r}) \right], \quad (1)$$

together with the equation $\mathbf{B} = \text{rot}\mathbf{A}$ and the definition of invariant Josephson phase $\varphi_{n,n+1} = \theta_{n+1} - \theta_n - \frac{2\pi}{\Phi_0} \int_{nd}^{(n+1)d} A_z dz$. Integrating \mathbf{A} over closed contour one obtains

$$\mathbf{B} \times \mathbf{z}_0 = \frac{\Phi_0}{2\pi d} \nabla_{\parallel}\varphi_{n,n+1} - \frac{4\pi\lambda^2}{cd} (\mathbf{j}_{n+1}^{\parallel} - \mathbf{j}_n^{\parallel}), \quad (2)$$

here \mathbf{B} is the averaged interlayer magnetic field, \mathbf{z}_0 is the unity vector perpendicular to the layer and d is the interlayer distance, layers assumed to be thin ($d \ll \lambda_L$).

Then, using Maxwell equation $\text{rot}\mathbf{B} = \frac{\epsilon}{c} \frac{\partial \mathbf{E}}{\partial t} + \frac{4\pi}{c} \mathbf{j}$, projected on to z-axes, we obtain

$$\frac{\epsilon}{c} \frac{\partial E_{n,n+1}}{\partial t} + \frac{4\pi}{c} j_{n,n+1} = \frac{\Phi_0}{2\pi d} \nabla_{\parallel}^2 \varphi_{n,n+1} - \frac{4\pi\lambda^2}{cd} \nabla_{\parallel} (\mathbf{j}_{n+1}^{\parallel} - \mathbf{j}_n^{\parallel}). \quad (3)$$

Taking use of the continuity equation $\frac{\partial \rho_n}{\partial t} + \nabla_{\parallel} \mathbf{j}_n^{\parallel} + \frac{j_{n,n+1} - j_{n-1,n}}{d_0} = 0$ and Maxwell equation $\epsilon \text{div}\mathbf{E} = 4\pi\rho$ in integral form $\rho_n = \frac{\epsilon}{4\pi d_0} (E_{n,n+1} - E_{n-1,n})$ one obtains finally the equation

$$\frac{c\Phi_0 d_0}{16\pi^2 \lambda^2} \nabla_{\parallel}^2 \varphi_{n,n+1} = \left(1 + \frac{dd_0}{2\lambda^2} \right) j_{n,n+1}^* - 0.5(j_{n-1,n}^* + j_{n+1,n+2}^*), \quad (4)$$

$$j_{n,n+1}^* = j_{n,n+1} + \frac{\epsilon}{4\pi} \frac{\partial E_{n,n+1}}{\partial t} - j_{ext} = j_{n,n+1} + \frac{\epsilon}{4\pi d} \frac{\partial V_{n,n+1}}{\partial t} - j_{ext}, \quad (5)$$

where j_{ext} is the external current in overlapping geometry (for the details of introducing the external current in different geometries see Ref. [7]).

To find the interlayer Josephson current $j_{n,n+1}$ we use the theory of nonequilibrium Josephson effect developed recently ([18, 19, 20, 21, 22, 23] and references therein). We take into account that in nonequilibrium state there is nonzero invariant potential

$$\Phi_n(t) = \phi_n + (\hbar/2e)(\partial\theta_n/\partial t), \quad (6)$$

where ϕ_n is the electrostatic potential and θ_n is the phase of superconducting condensate, $\Phi = 0$ in the equilibrium state.

An ordinary Josephson relation $(d\varphi/dt) = (2e/\hbar)V$ between the Josephson phase difference $\varphi_{n,n+1}$ and voltage $V_{n,n+1} = E_{n,n+1}d$ is violated. Instead, we have (from (6))

$$\frac{\partial \varphi_{n,n+1}}{\partial t} = \frac{2e}{\hbar} V_{n,n+1} + \frac{2e}{\hbar} (\Phi_{n+1} - \Phi_n). \quad (7)$$

The charge density inside a superconducting layer is

$$\rho_n = -2e^2 N_0 (\Phi_n - \Psi_n), \quad (8)$$

where the first term is the charge of superconducting electrons determined by the shift of the condensate chemical potential $\delta\mu_s = -e\Phi$ and the second term is the quasiparticle charge, described by potential Ψ_n (details can be found in Ref. [23]). Finally, the equation for the charge imbalance can be written in the form corresponding to the generalized nonstationary Ginzburg-Landau theory [23]

$$\frac{\partial \Psi_i}{\partial t} = (1 - \Gamma) \frac{\partial \Phi_i}{\partial t} + 2\nu_t \frac{\hbar}{2e} \left(\frac{\partial \varphi_{i-1,i}}{\partial t} - \frac{\partial \varphi_{i,i+1}}{\partial t} \right) + 2\nu_t (\Psi_{i-1} + \Psi_{i+1} - 2\Psi_i) - \tau_q^{-1} \Psi_i, \quad (9)$$

where $\eta = 2\nu_t \tau_q$ is the parameter of disequilibrium, τ_q is the well-known charge-imbalance relaxation time, $\nu_t = (4e^2 N_0 R S d_0)^{-1}$ is the "tunnel frequency", R is the normal resistivity of the tunnel junction, $V = S d_0$ is the volume of the superconducting layer, $N_0 = m p_F / 2\pi^2 \hbar^3$ is the density of state (or, instead, $N_f = N_0 d_0$ can be considered as 2D density of states), $\Gamma \ll 1$ is the parameter dependent on the details of microscopic theory.

In the same approximation we derive the expression for the nonequilibrium interlayer current [23]

$$j_{i,i+1} = j_c \sin \varphi_{i,i+1} + \frac{\hbar}{2eR} \frac{\partial \varphi_{i,i+1}}{\partial t} + \frac{\Psi_i - \Psi_{i+1}}{R}. \quad (10)$$

Finally, in dimensionless form we obtain

$$\nabla_{\parallel}^2 \varphi_{i,i+1} = j_{i,i+1}^* - s(j_{i-1,i}^* + j_{i+1,i+2}^*), \quad (11)$$

$$j_{i,i+1}^* = \beta \frac{\partial^2 \varphi_{i,i+1}}{\partial \tau^2} + \frac{\partial \varphi_{i,i+1}}{\partial \tau} + \sin \varphi_{i,i+1} + \psi_i - \psi_{i+1} + \beta \left(\frac{\partial \mu_i}{\partial \tau} - \frac{\partial \mu_{i+1}}{\partial \tau} \right) - j_{ext}, \quad (12)$$

$$\alpha' \frac{\partial \psi_i}{\partial \tau} + \psi_i + \eta (2\psi_i - \psi_{i-1} - \psi_{i+1}) = \eta \left(\frac{\partial \varphi_{i-1,i}}{\partial \tau} - \frac{\partial \varphi_{i,i+1}}{\partial \tau} \right) + \alpha' (1 - \Gamma) \frac{\partial \mu_i}{\partial \tau}, \quad (13)$$

$$\mu_i + \zeta (2\mu_i - \mu_{i-1} - \mu_{i+1}) = \psi_i + \zeta \left(\frac{\partial \varphi_{i-1,i}}{\partial \tau} - \frac{\partial \varphi_{i,i+1}}{\partial \tau} \right). \quad (14)$$

where $\mu(t) = \Phi(t)/V_c$, $\psi(t) = \Psi(t)/V_c$, $V_c = \hbar \omega_c / 2e$, $\alpha' = \tau_q \omega_c$, $\beta = (\hbar \epsilon \omega_c^2 S) / (8\pi e d j_c)$, $\lambda_J^2 = (\hbar c^2 d_0) / (16\pi e j_c (\lambda^2 + d d_0))$, $\zeta = (\epsilon r_d^2) / (d_0 d)$, $\omega_c = 2e R j_c / \hbar$, $\tau = \omega_c t$, $\tilde{x} = x / \lambda_J$, $s = 0.5 / (1 + (d d_0) / (2\lambda^2))$.

This system of equations is a generalization of well-known magnetic coupling model of layered superconductors [7, 8]. Neglecting electron-hole imbalance ($\eta = 0$, $\Psi_n = 0$), we

derive the system of equations obtained in Ref. [15], and neglecting the charge effect ($\zeta = 0$, $\Psi_n = \Phi_n$) we derive the system of equations similar to that of [18, 19, 24].

Before further study, the Eqs. (11)-(14) must be added with boundary conditions, which we write as

$$\begin{aligned}
j_{-1,0}^* &= j_{N,N+1}^* = 0, \\
\left. \frac{\partial \varphi_{i,i+1}}{\partial x} \right|_{0,L} &= B, \\
\psi_0 &= \psi_N = 0, \\
\left. \frac{\partial \psi_{i,i+1}}{\partial x} \right|_{0,L} &= 0, \\
\mu_0 &= \mu_N = 0.
\end{aligned} \tag{15}$$

For numerical solution of the equations (11)-(14) with boundary conditions (15) we introduce the new functions $\hat{\varphi}$, v , z , defined by the relations

$$\begin{aligned}
\hat{\varphi}_i(x, t) &= \varphi_{i,i+1}(x, t) - Bx, \\
v_i(x, t) &= \frac{\partial \hat{\varphi}_i(x, t)}{\partial t} + \psi_i(x, t) - \psi_{i+1}(x, t), \\
z_i(x, t) &= \varepsilon \frac{\partial \hat{\varphi}_i(x, t)}{\partial t} + \alpha'(\psi_i(x, t) - \psi_{i+1}(x, t)), \\
i &= 0, \dots, N-1, \quad \varepsilon = \alpha'(1 - \Gamma).
\end{aligned} \tag{16}$$

Let us denote now by U the column vector-function of kind

$$U = \begin{pmatrix} \hat{\varphi} \\ v \\ z \end{pmatrix}, \tag{17}$$

by \hat{A} the operator matrix of kind

$$\hat{A} = \begin{pmatrix} 0 & \frac{\alpha'\beta}{\alpha'-\varepsilon} & -\frac{\beta}{\alpha'-\varepsilon} \\ 0 & -1 + \zeta \Delta_d & 0 \\ 0 & -\varepsilon(1 - \frac{\beta}{\alpha'-\varepsilon}) - \frac{\beta\gamma\varepsilon}{\alpha'-\varepsilon} \nabla_{\parallel}^2 + \beta\eta \Delta_d & \frac{\beta\gamma}{\alpha'-\varepsilon} \nabla_{\parallel}^2 - \frac{\beta}{\alpha'-\varepsilon} \end{pmatrix}, \tag{18}$$

(here Δ_d is the difference Laplasian, $(\Delta_d f)_i = f_{i-1} - 2f_i + f_{i+1}$) and by F the column vector of kind

$$F = \begin{pmatrix} 0 \\ (1 - \zeta \Delta_d)(j^* + j_{ext} - \sin(\varphi)) \\ \varepsilon(j^* + j_{ext} - \sin(\varphi)) \end{pmatrix}. \tag{19}$$

Then we can rewrite the above system of equations in the following "operator" form:

$$\begin{aligned}\beta \frac{\partial U}{\partial t} &= \hat{A}U + F, \\ (s\Delta_d + 2s - 1)j^* &= -\nabla_{\parallel}^2 \hat{\varphi},\end{aligned}\tag{20}$$

with appropriate homogeneous boundary conditions. For numerical solution of the equation (20) we use, after sampling in x -direction, the semi-implicit scheme of form

$$U(t + \Delta t) = 2\left(E - \frac{\Delta t}{2\beta}\hat{A}\right)^{-1}\left(U(t) + \frac{\Delta t}{\beta}F(t)\right) - U(t) - \frac{\Delta t}{\beta}F(t),\tag{21}$$

in which all needed inverse operators can be easily evaluated by standard sweep method. The transformation from vector U to initial variables is evident.

The developed program gives us the possibility to observe the state of system during calculation process in convenient graphical form. We can therefore find many different variants of system dynamics and vortex lattice structures.

The most part of simulations has been carried out for the case of high magnetic fields $H > H^* = \Phi_0/\gamma t^2$, where $\Phi_0 = \pi\hbar c/e$ is the flux quantum, $\gamma = \lambda_c/\lambda_{ab}$ is the anisotropy parameter, and $t = d + d_0$ is the period of the structure. At this fields triangular vortex lattice is formed in the static case.

The results of numerical simulations can be shortly described in the following way. At small currents vortex lattice remains triangular. At high currents the situation depends on dissipation. If interlayer dissipation is strong enough ($\beta < 1$) then triangular lattice is stable at all currents. Otherwise, we observed various transformations of lattice structure (further $\beta = 100$ and $s = 0.48$ are considered).

(i) At pure magnetic coupling ($\zeta = 0$, $\eta = 0$) we obtain the typical picture of JVL transformations. The example is shown on Fig. 1. We consecutively change current from zero to some high value ($a-f$) and then decrease it up to zero again ($g-l$). The square lattice is clear seen on Fig. d, e, i , and j . Low current regimes a, l , as well as high current one f, g are triangular (or close to it). Regimes b, c and k are "inhomogeneous", – velocities of vortex chains are different in different layers. These regimes are also "breathing" due to strongly excited nonlinear plasma waves. We find that such breathing modes can be triangular or square in average. Note that different regimes exist at the same current that can lead to hysteresis on VCC.

(ii) If we take charge coupling into account (Fig. 2, $\zeta = 1$, $\eta = 0$), the picture of JVL

transformations is qualitatively the same but the regimes with square lattice are shifted to higher currents.

(iii) For charge-imbalance (quasiparticle) coupling the result is qualitatively different. We have found that if the time of charge-imbalance relaxation is large enough (approximately $\alpha' = \tau_q \omega_c > 1$) than the triangular lattice become stable even if the parameter of disequilibrium η is small. The example is shown on Fig.3 ($\zeta = 0.1, \eta = 0.1, \alpha' = 100$). There is no JVL transformations at this parameters although both charge and charge-imbalance couplings are weak. The origin of this effect is the additional dissipation due to the charge-imbalance relaxation. The detailed theory will be considered in other publication.

In conclusion, we derive macroscopic dynamical equations for layered superconductors with magnetic, charge and nonequilibrium quasiparticle interactions taken into account. Many dynamical regimes are observed, in particular triangular, square, inhomogeneous and breathing modes. We established that additional dissipation due to the charge-imbalance relaxation can prevent JVL transformations and make triangular lattice stable at all currents.

This work is supported by the Russian Foundation for Basic Research, Grants No. 00-02-16528, 99-02-16188 and 00-15-96734 ("Leading Scientific Schools"). The authors thanks Prof. A. Andronov, Prof. J. Keller, Prof. R. Kleiner, Dr. V. Kurin, Dr. A. Mel'nikov, and Dr. Ch. Preis for valuable discussions.

-
- [1] J. Lee, J. Nordman, and G. Hohenwarter, Appl. Phys. Lett. **67**, 1471 (1995).
 - [2] J. Lee *et al.*, Appl. Phys. Lett. **71**, 1412 (1997).
 - [3] A. Irie, Y. Hirai, and G. Oya, Appl. Phys. Lett. **72**, 2159 (1998).
 - [4] V. Krasnov, N. Mros, A. Yurgens, and D. Winkler, Phys. Rev. B **59**, 8463 (1999).
 - [5] G. Hechtfischer *et al.*, Phys. Rev. B **55**, 14638 (1997).
 - [6] G. Hechtfischer, R. Kleiner, A. Ustinov, and P. Muller, Phys. Rev. Lett. **79**, 1365 (1997).
 - [7] S. Sakai, P. Bodin, and N. Pedersen, J. Appl. Phys. **73**, 2411 (1993).
 - [8] L. Bulaevskii *et al.*, Phys. Rev. B **50**, 12831 (1994).
 - [9] R. Kleiner *et al.*, Phys. Rev. B **50**, 3942 (1994).
 - [10] R. Kleiner, Phys. Rev. B **50**, 6919 (1994).
 - [11] A. Ustinov and H. Kohlstedt, Phys. Rev. B **54**, 6111 (1996).

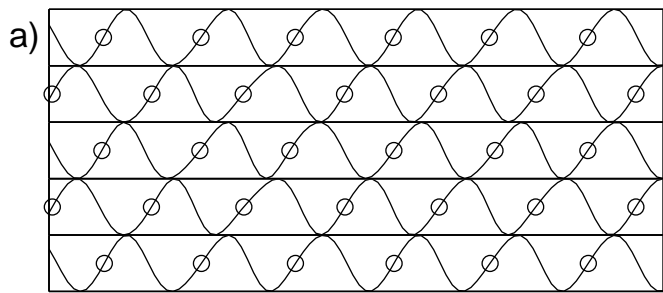
- [12] S. Artemenko and S. Remizov, JETP Letters **66**, 853 (1997), [Pis'ma Zh. Eksp. Teor. Fiz. **66**, 811 (1997)].
- [13] A. Ustinov and S. Sakai, Appl. Phys. Lett. **73**, 686 (1998).
- [14] A. Volkov and V. Glen, J. of Phys.: Cond. Matt. **10**, L563 (1998).
- [15] M. Machida, T. Koyama, A. Tanaka, and M. Tachiki, PHYSICA C **330**, 85 (2000).
- [16] A. E. Koshelev and I. S. Aranson, Phys. Rev. Lett **85**, 3938 (2000).
- [17] R. Kleiner, T. Gaber, and G. Hechtfisher, Phys. Rev. B **62**, 4086 (2000); R. Kleiner, T. Gaber, and G. Hechtfisher, unpublished.
- [18] L. Bulaevskii *et al.*, Phys. Rev. B **53**, 14601 (1996).
- [19] L. Bulaevskii *et al.*, Phys. Rev. B **54**, 7521 (1996).
- [20] T. Koyama and M. Tachiki, Phys. Rev. B **54**, 16183 (1996).
- [21] S. Artemenko and A. Kobelkov, Phys. Rev. Lett. **78**, 3551 (1997).
- [22] D. Ryndyk, Phys. Rev. Lett. **80**, 3376 (1998).
- [23] D. Ryndyk, JETP **89**, 975 (1999), [Zh. Eksp. Teor. Fiz. **116**, 1798 (1999)].
- [24] A. Mel'nikov, Phys. Rev. Lett. **77**, 2786-2789 (1996).

Figure captions

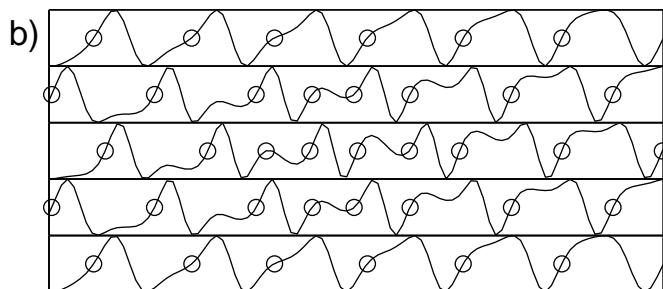
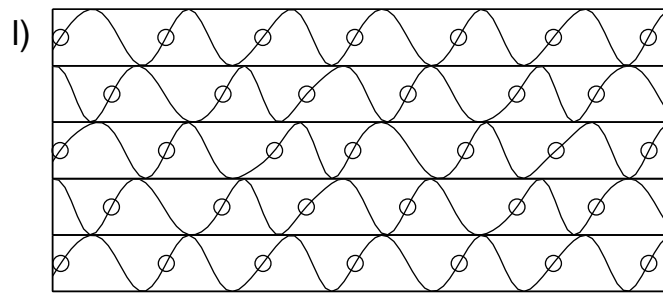
Fig.1. The structure of Josephson vortex lattice ($\sin \varphi_n$ are shown) with $\beta = 100$, $s = 0.48$, $\eta = 0$, $\zeta = 0$, $j = 0.2, 0.4, 0.6, 0.8, 1, 1.2$. Current is increased (*a-f*) and then decreased (*g-l*).

Fig.2. The structure of Josephson vortex lattice with $\beta = 100$, $s = 0.48$, $\eta = 0$, $\zeta = 1$.

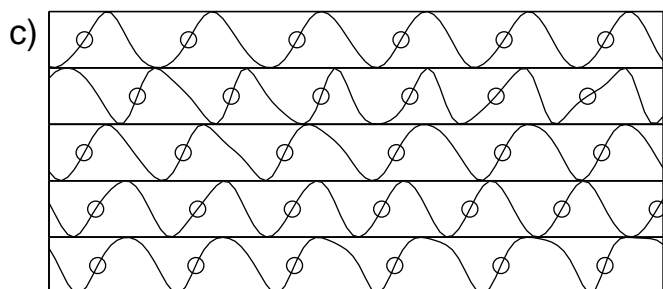
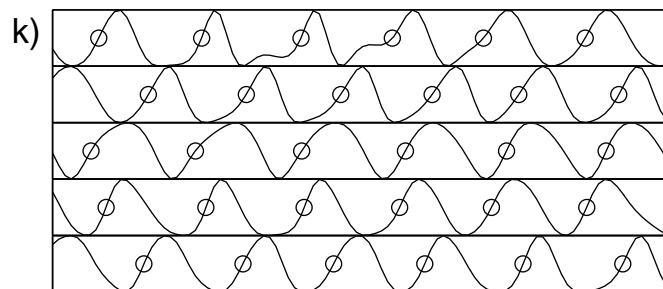
Fig.3. The structure of Josephson vortex lattice with $\beta = 100$, $s = 0.48$, $\eta = 0.1$, $\zeta = 0.1$, $\alpha' = 100$, $\Gamma = 0.01$.



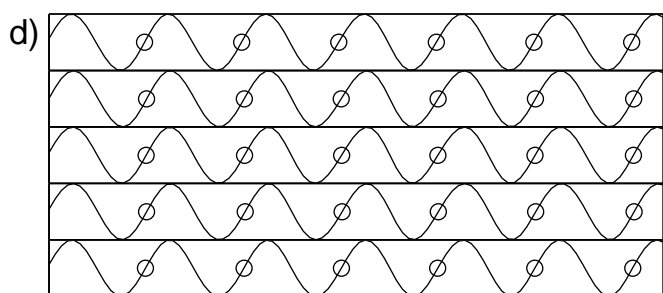
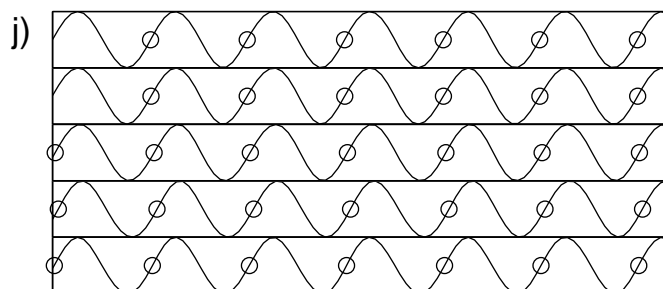
$j=0.2$



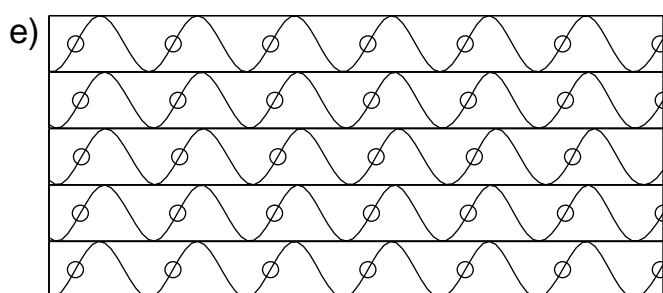
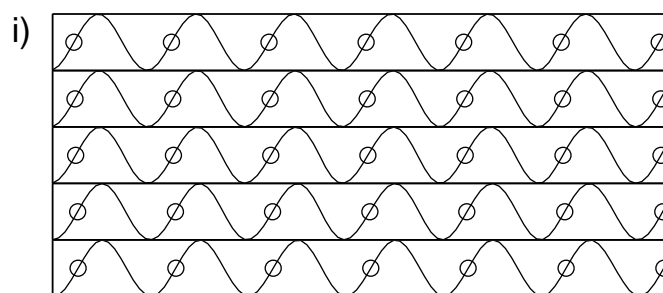
$j=0.4$



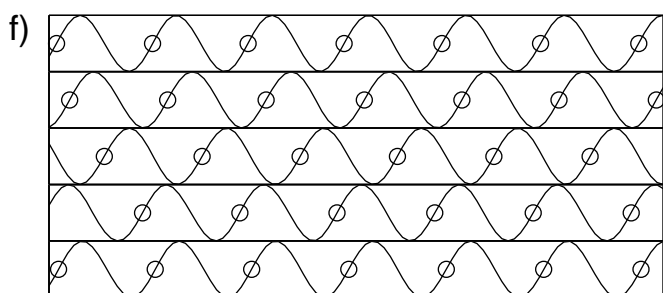
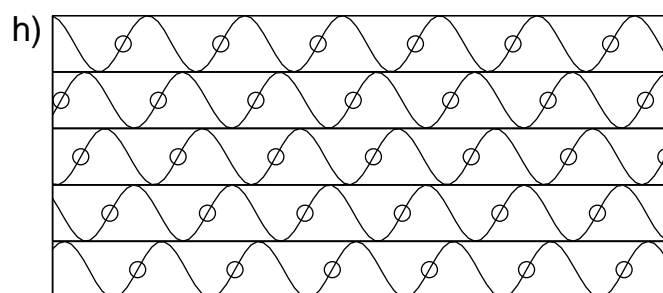
$j=0.6$



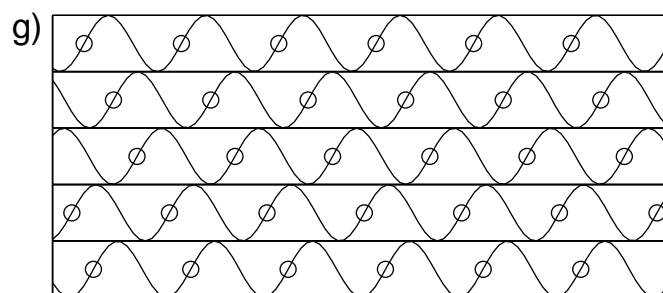
$j=0.8$

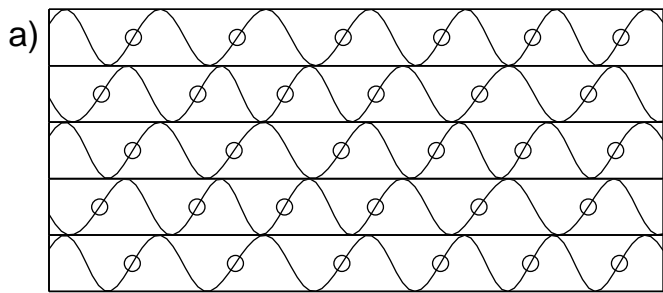


$j=1$

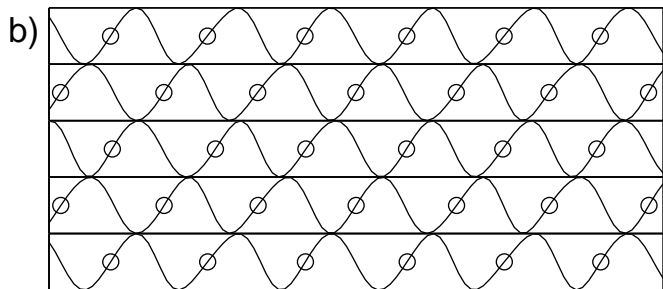
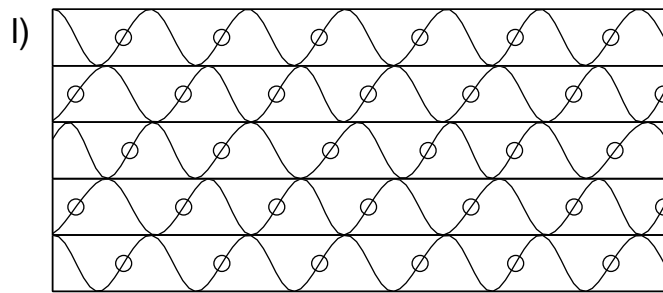


$j=1.2$

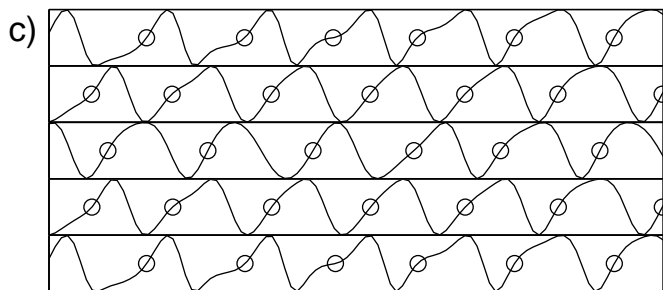
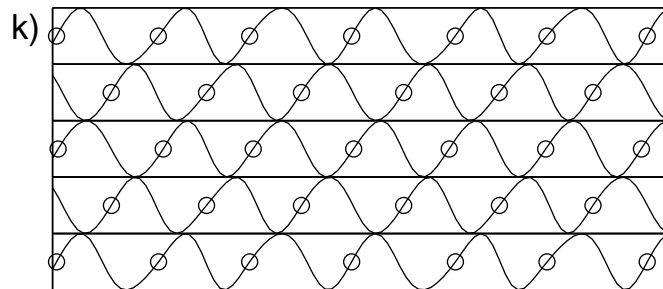




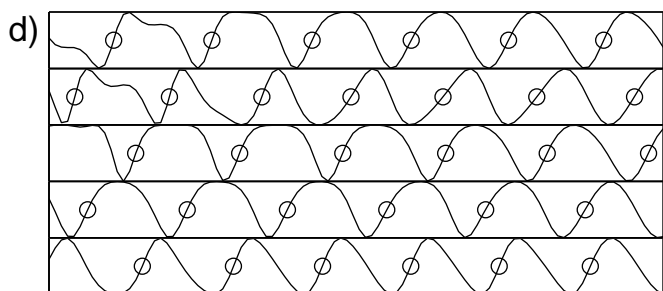
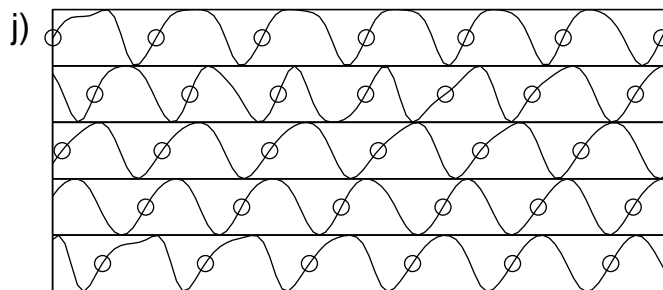
$j=0.2$



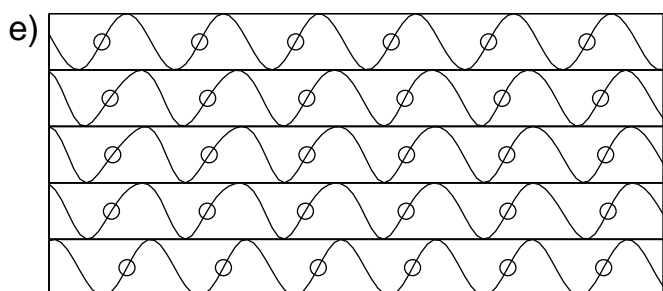
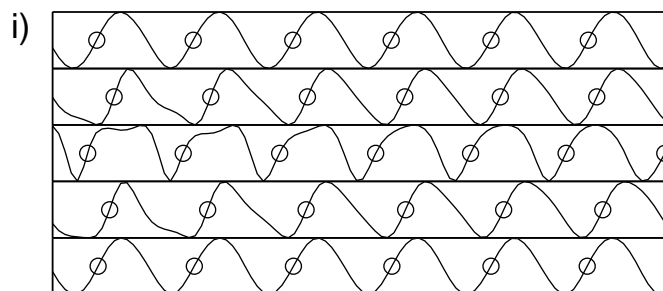
$j=0.4$



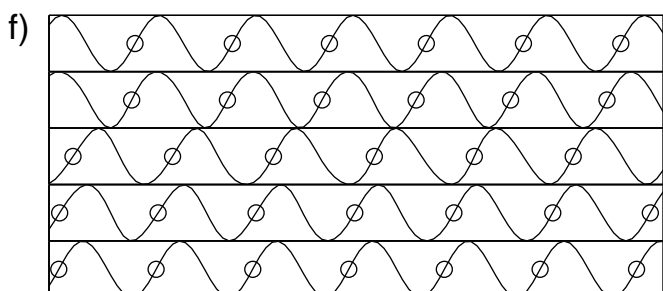
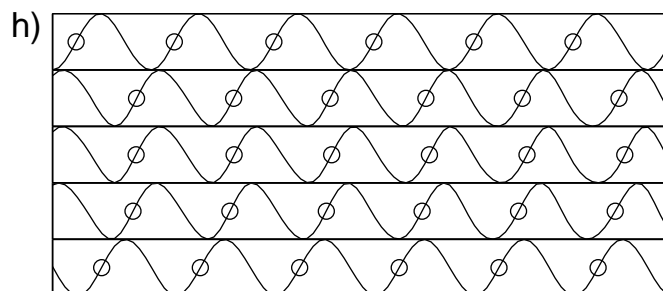
$j=0.6$



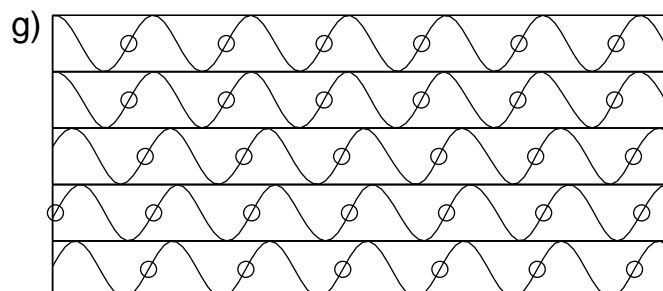
$j=0.8$

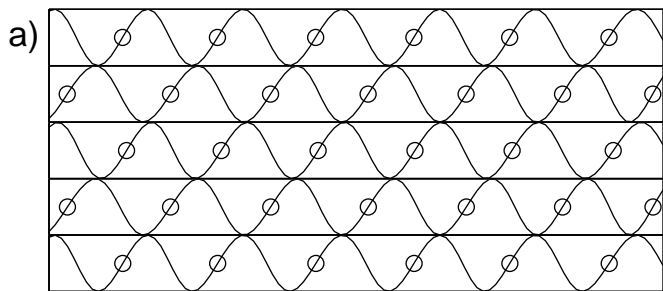


$j=1$

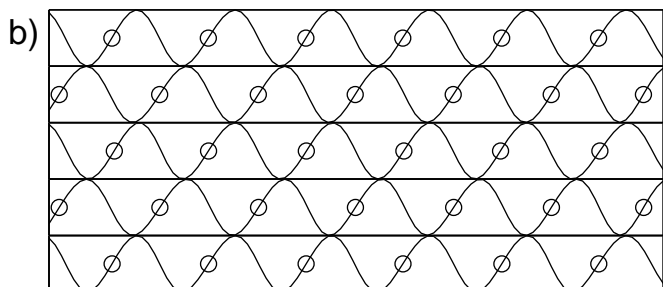
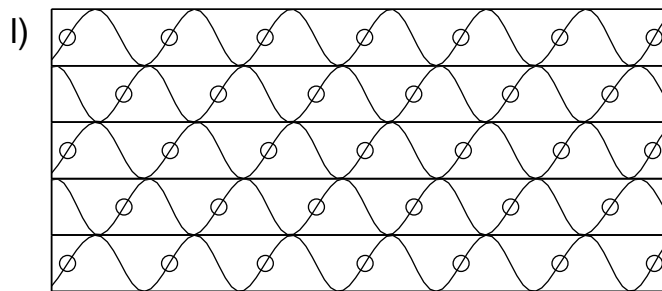


$j=1.2$

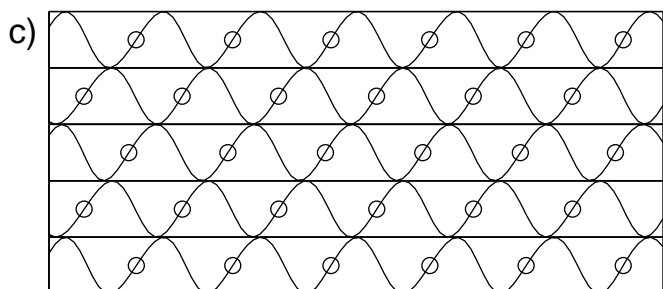
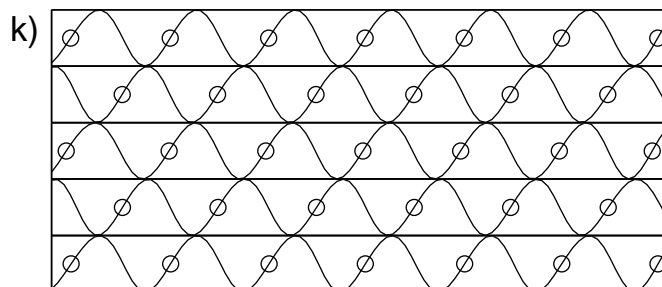




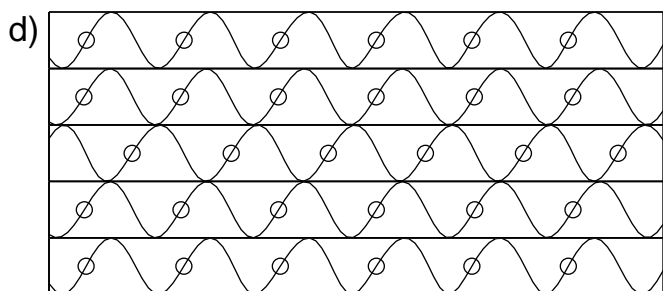
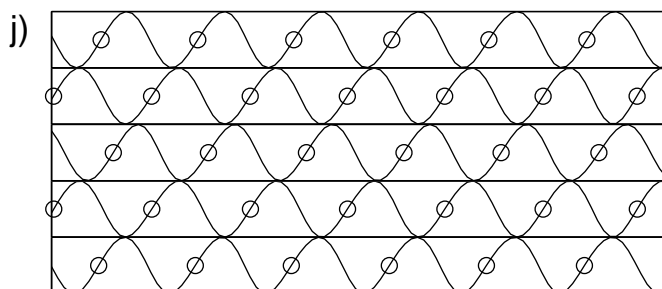
$j=0.2$



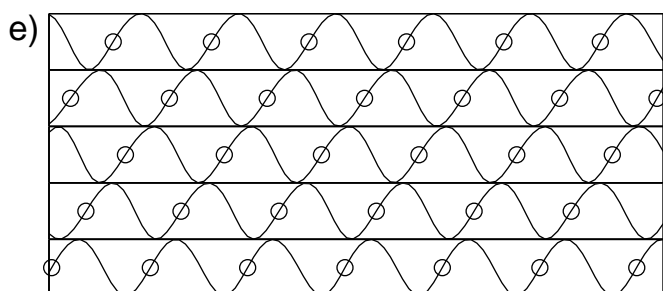
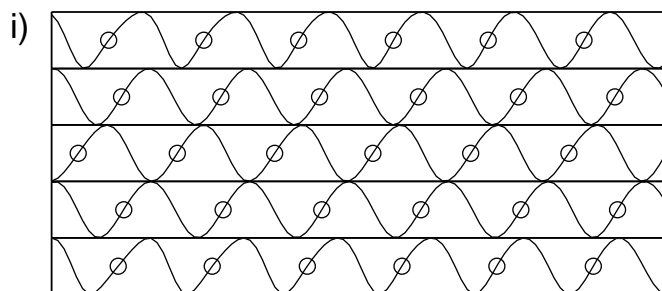
$j=0.4$



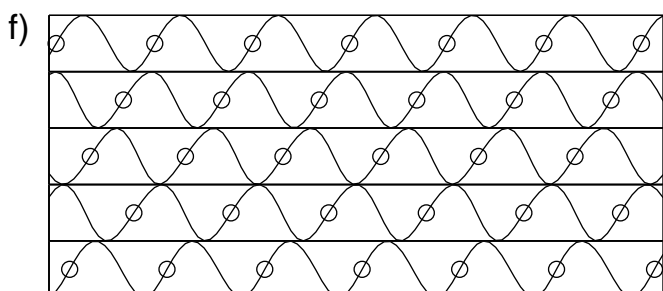
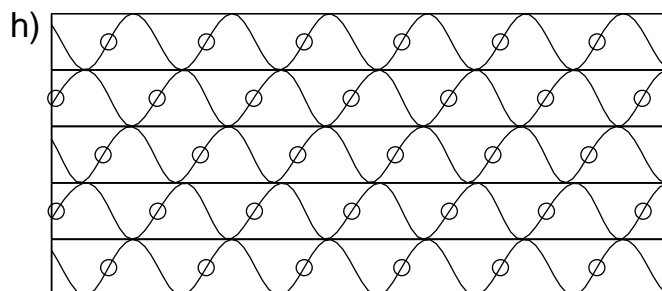
$j=0.6$



$j=0.8$



$j=1$



$j=1.2$

